Edge-flames and Cellular Structures in Oscillatory Non-premixed Counterflows

D.A.Kessler[1], M.Short[1], J.Buckmaster[2]
University of Illinois at Urbana-Champaign
[1]Department of Theoretical and Applied Mechanics
[2]Department of Aerospace Engineering
Urbana, IL, USA
Corresponding Author, D.A.Kessler: dakessle@uiuc.edu

Introduction

In the following we study the evolution of an edge-flame in an oscillatory, symmetric non-premixed counterflow. An edge-flame can be thought of as a two-dimensional transition between any two permissible states for a particular set of flame parameters (Buckmaster 2002). The most common method of constructing edge-flames is to establish a one-dimensional flame in a counterflow configuration for which two different stable solutions are admissible and then seek a two-dimensional structure that can serve as a transition between these two solutions. The dynamics of edge-flames in unsteady flows are of particular interest in the study of turbulent combustion (Kessler et al. 2005), where the turbulent flow continuously tears and disrupts the flame sheet, continuously forming edge-flames. In order to understand how edge-flames may respond to an unsteady flow, we will study the response of a non-premixed edge flame to an unsteady straining flow in a symmetric counterflow configuration. Earlier work that examines the effect of unsteady straining flows on 1-dimensional flames (premixed and non-premixed) can be found (McIntosh et al. 2001; Sung and Law 2000; Egolfopoulos 2000; Huang et al. 1998; Echekki and Chen 1996), while a 2-D study of edge-flames in an oscillatory premixed counterflow has been presented (Kessler et al. 2005).

The edge-flame configuration

Apart from the fact that the flow field is unsteady, the formulation is that of Short et al. (2001). Assuming a 1-step Arrhenius kinetic model and a constant density approximation, the equations to be solved in their non-dimensional form are then

$$\begin{aligned} X_t &= -uX_x + Le_X^{-1}(X_{xx} + X_{zz}) - \alpha_X Y_\infty DXY e^{-\frac{\theta}{T}}, \\ Y_t &= -uY_x + Le_Y^{-1}(Y_{xx} + Y_{zz}) - \alpha_Y X_\infty DXY e^{-\frac{\theta}{T}}, \\ T_t &= -uT_x + T_{xx} + T_{zz} + qDYe^{-\frac{\theta}{T}}, \end{aligned} \tag{1}$$

where the magnitude of the temporally oscillating straining flow is determined from

$$u = -x(1 - A\sin\omega t). \tag{2}$$

Here T is the temperature, Y is the mass fraction of fuel, X is the mass fraction of oxidizer, q is the nondimensional heat release rate, θ is the nondimensional activation energy, D is the Damkohler number, and $\alpha_X Y_\infty$ and $\alpha_Y X_\infty$ are the stoichiometric coefficients. The boundary conditions are:

$$T \to T_f, Y \to 1, X \to 0 \text{ as } x \to +\infty; \quad T \to T_f, Y \to 0, X \to 1 \text{ as } x \to -\infty; \tag{3}$$

$$T_z,\ Y_z,\ X_z \rightarrow\ 0 \text{ as } |z| \rightarrow \infty. \tag{4}$$

The first and second of these, (3), specify the cold supply conditions on the fuel and oxidizer supply side. Suitable initial conditions lead to edge-flame solutions, transitions between strong burning as $z \rightarrow \infty$ and a quenched state ($T = T_f, X = 1, Y = 1$) as $z \rightarrow -\infty$, and are established in the usual way (Short et al. 2001). In this study we examine the overall reaction,

$$H_2 + O_2/2 \rightarrow H_2O \tag{5}$$

We will assume that the oxidizer stream is air, and thus $X_\infty = 0.22$, while $Y_\infty = 0.01$ representing a fuel supply stream consisting of 14% H_2 diluted in nitrogen gas. The stoichiometric ratio for the supply streams is then $\alpha_X Y_\infty / \alpha_Y X_\infty = 0.36$. For the calculations presented herein, we take $q = 1.2$, $T_\infty = 0.2$, and $\theta = 8.0$. If $T_\infty = 0.2$ is equivalent to 300K, then a flame temperature of $T = 1.0$ would correspond to a dimensional temperature of 1500K. The Lewis numbers of the fuel and oxidizer are $Le_Y = 0.3$ and $Le_X = 1.0$, respectively. We also consider a binary reaction in which the Lewis numbers of the fuel and oxidizer are both equal to unity as are $\alpha_x Y_\infty$ and $\alpha_y X_\infty$. This model flame will help to accentuate the role of the Lewis number in edge-flame instabilities. This set of equations is solved using fourth-order finite differencing in space, and a high-order Runge-Kutta time integration technique. We will present results in terms of a scaled Damkohler number,

$$D = \overline{D}\theta^2 \exp(\theta/T_a) \tag{6}$$

where T_a is the adiabatic flame temperature taken to be 0.6 in these calculations.

Results

Le=0.3

We begin by examining how the range of $\overline{D}$ for which it is possible for cellular edge-flame instabilities to exist is affected by the presence of the unsteady forcing. It was found that in the case of a steady counterflow (Short et al. 2001), cellular structures form when $\overline{D}$ lies in the interval $\overline{D}_E < \overline{D} < \overline{D}_C$ where $\overline{D}_E \approx 0.0046$ and $\overline{D}_C \approx 0.0049$. In the presence of an unsteady straining flow, this range of $\overline{D}$ is much broader. Figure 1 shows a series of plots in the forcing flow amplitude A and frequency ω plane for various $\overline{D}$ that identify cellular instability boundaries. The term extinguished refers to the dynamic failure of the trailing 1-D flame and subsequent failure of the edge-flame itself, while propagating flame refers to an edge-flame trailing a stable one-dimensional configuration. It is clear from figure 1 that cellular edge-flame structures can persist for $\overline{D}$ as large as 0.0065. The nature of the cellular instability observed in the presence of the time-periodic straining field is sensitive to the frequency and amplitude of the forcing. Two types are shown in figs. 2 and 3. Figure 2 shows a time sequence of temperature contours within the domain for $\overline{D} = 0.005$ forced at the frequency $\omega = 0.5$. A flame-string is formed initially (Buckmaster 1992) that stretches, splits into two flame strings, which drift but do not seem to be able to split again within the finite domain. Figure 3 shows a sequence of temperature contours for $\overline{D} = 0.0065$ forced with the frequency, $\omega = 1$. In this example, the flame string dynmaics are similar to the previous case for the six time frames. Subsequently, both flame strings split to form a warp of four flame strings reminiscent of the cellular structures found in Short et al. (2001). Note that the

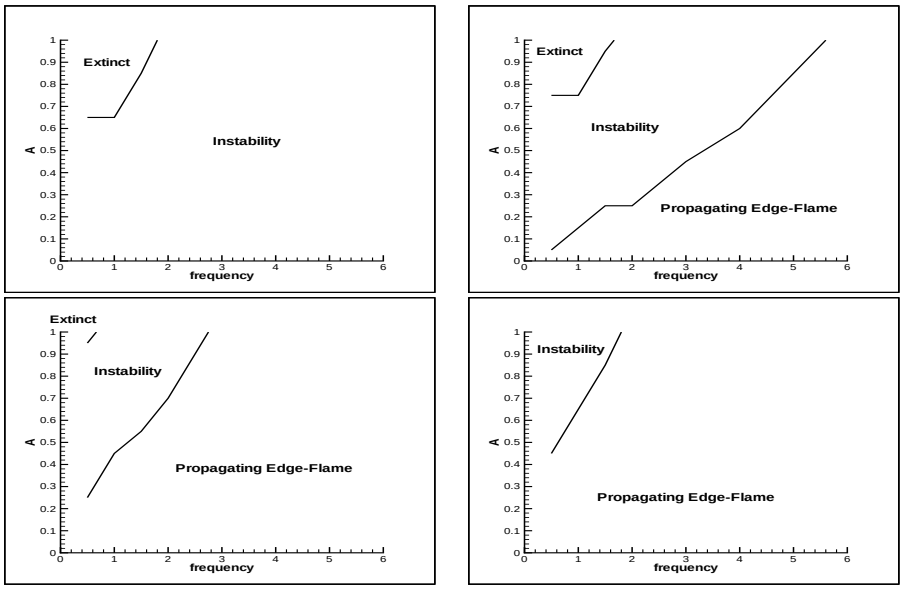

Figure 1: Stability Boundaries for (from left to right) $\overline{D}$ =0.0047, 0.0050, 0.0058, 0.0065

values of $\overline{D}$ used in figures 2 and 3 correspond to a $\overline{D}$ for which stable edge-flame solutions exist for the steady counterflow configuration. The existence of sublimit flame strings for $\overline{D} < \overline{D}_e$ were noted in Short et al. (2001) for the analagous steady counterflow configuration. In this work, we note the dynamic behavior of these flame strings to the unsteady counterflow. Contours of the flame temperature for a representative flame string configuration are given in figure 4. The response at this $\overline{D}$ in the steady counterflow configuration is a set of three stationary flame strings. In this case, however, we notice that the two flame strings located nearest to the boundary at $z = 20$ extinguish leaving behind a single stationary flame string. Other responses can be obtained by varying A and will be discussed more extensively during the oral presentation.

In Short et al. (2001), it was noted that in a steady counterflow, the amount of fuel available in the supply stream plays a role in whether cellular structures can form. While finding various examples of cellular structures for $\alpha_x Y_\infty = 0.5$ and 0.75, no such examples were found for $\alpha_x Y_\infty = 1.0$ when the counterflow is steady. We present an example of such a cellular structure formed in response to unsteady focing with $A = 0.9$ and $\omega = 5.0$ in figure 5.

We now turn our attention to values of $\overline{D}$ sufficiently large such that the trailing 1-D flame persists regardless of the values of A and ω. It has been well documented that edge-flames travel at a well-defined speed dependent on $\overline{D}$ for the steady counterflow configuration. We wish to examine the response of the mean edge speed to the frequency and amplitude of the forcing in such cases. We characterize the position of the edge flame as the location in the x-z plane of the maximimum reaction rate. This quantity is charted with time for the various A, ω combinations tested. Due to the symmetric nature of the sinusoidal forcing function, the location of the x-coordinate of the reaction rate remains essentially constant with time, so we present the variation of the z-coordinate as a function of time. It is clear from Figure 6 that both A and ω affect the mean motion of the edge flame for $\overline{D} = 0.0090$.

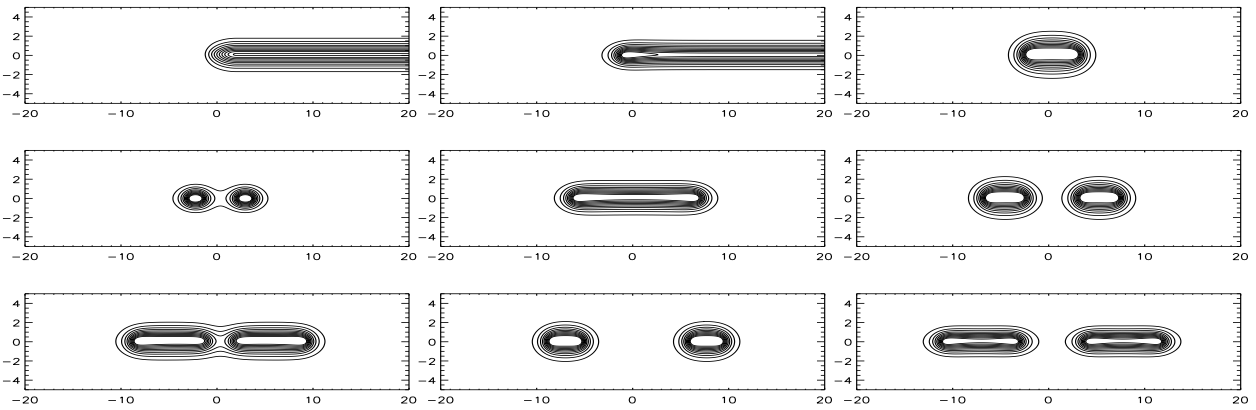

Figure 2: Temperature contours in the $(z - x)$ plane for $\overline{D} = .0050$, $A = 0.5$, $Le_Y = .3$, $\omega = 0.5$; contour levels .2,1.2(.1). The times for the panels are $t = 0$ to $t = 64$ incremented by 8. Panels ordered from left to right.

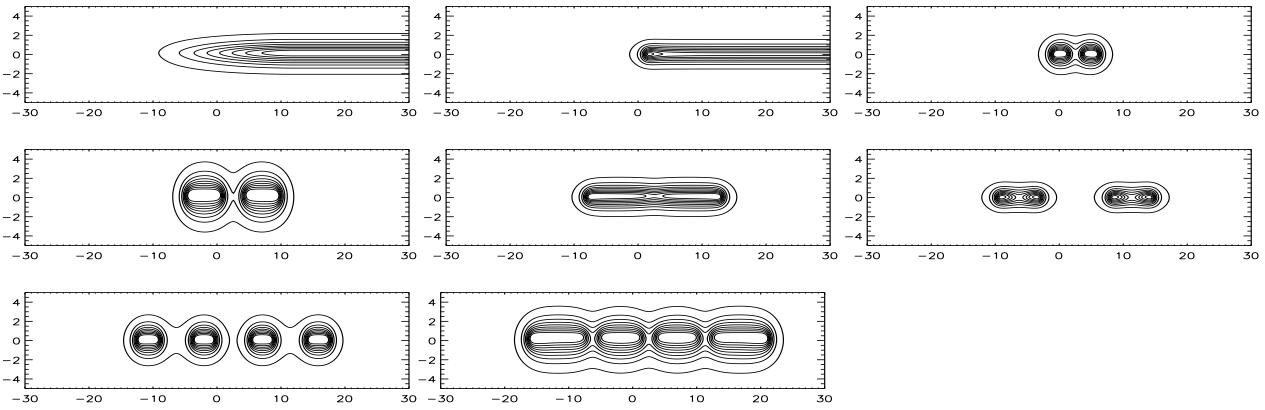

Figure 3: Temperature contours in the (z, x) plane for $\overline{D} = .0065$, $A = 0.9$, $Le_Y = .3$, $\omega = 1$; contour levels .2,1.2(.1). The panels are ordered as in Figure 2.

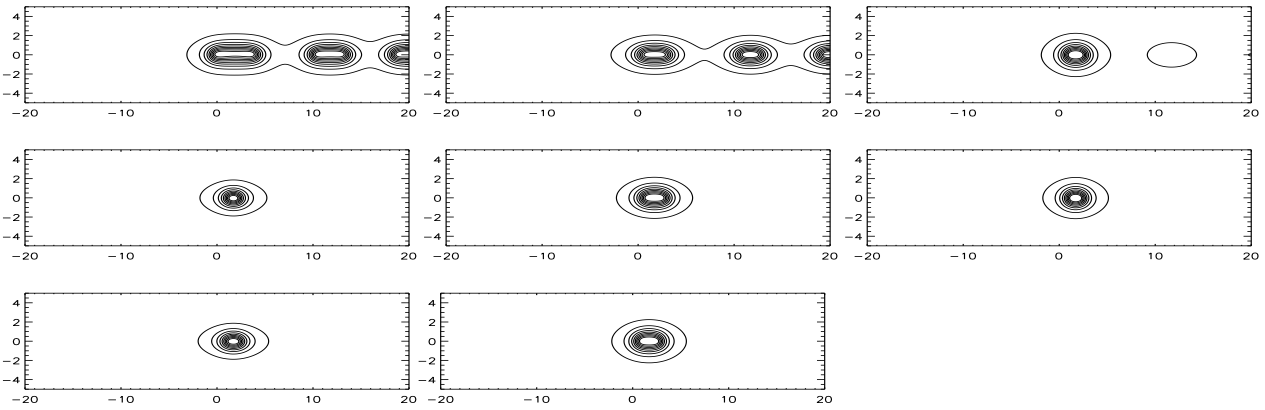

Figure 4: Temperature contours in the (z, x) plane for $\overline{D} = .00325$, $A = 0.25$, $Le_Y = .3$, $\omega = 1$; contour levels .2,1.4(.1). The times for the panels are $t = 0$ to $t = 28$ incremented by 4. The panels are ordered as in Figure 2.

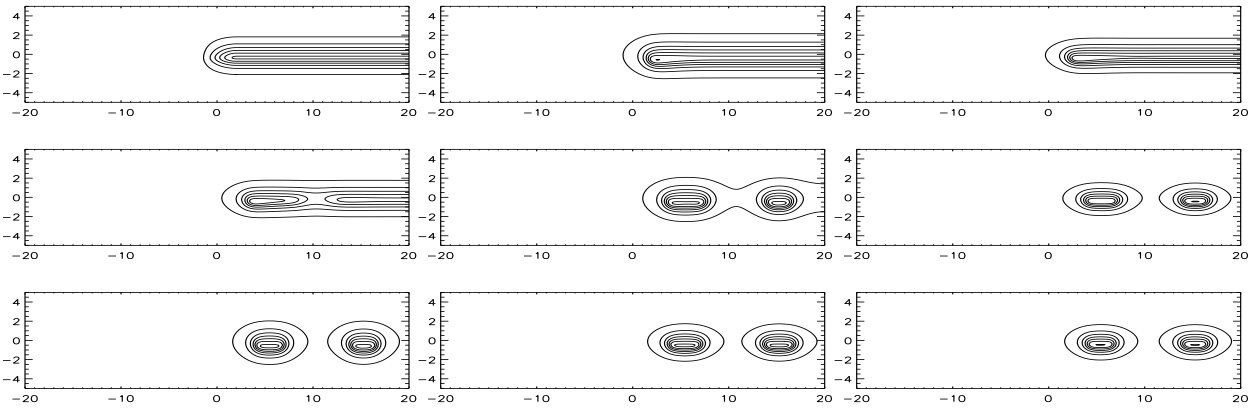

Figure 5: Temperature contours in the (z, x) plane for $\overline{D} = .055$, $A = 0.9$, $Le_Y = .3$, $\omega = 5$ $\alpha_x Y_\infty = 1.0$; contour levels .2,1.2(.1). The times for the panels are $t = 0$ to $t = 48$ incremented by 6. The panels are ordered as in Figure 2.

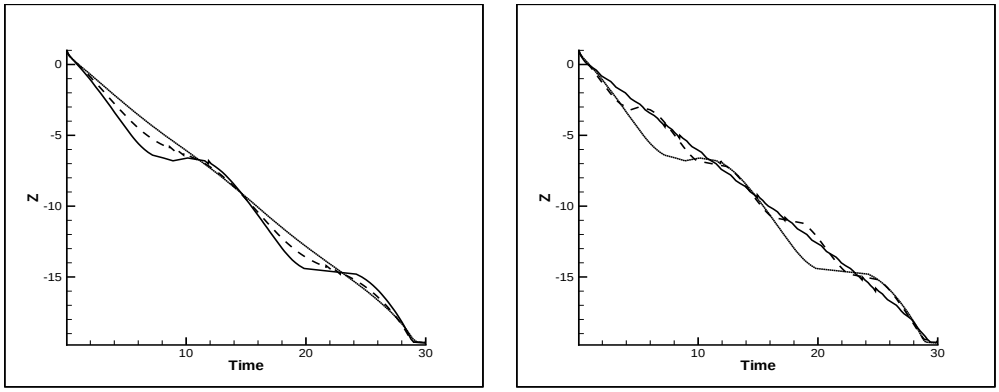

Figure 6: z-coordinate of Maximum Reaction Rate in Domain as a Function of Time for $\overline{D} = 0.0090$, $Le_Y = 0.3$, a.) $\omega = 0.5$, $A = 0.1$ (dotted), $A = 0.5$ (dashed), $A = 1.0$ (solid). b). $A = 1.0$, $\omega = 0.5$ (dotted), $\omega = 1.0$ (dashed), $\omega = 5.0$ (solid).

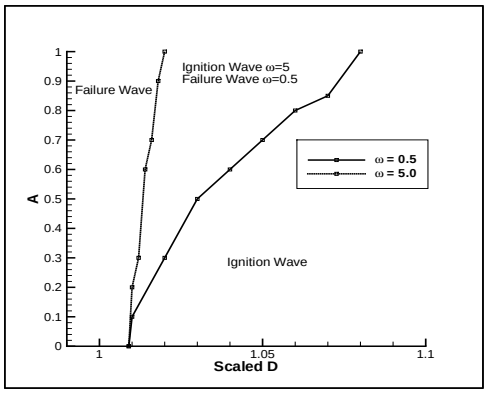

Figure 7: Boundary Between Propagating and Retreating Edge-Flames as a function of the Amplitude of Forcing and the Damkohler number for $\omega = 0.5$ (solid) and $\omega = 5.0$ (dotted)

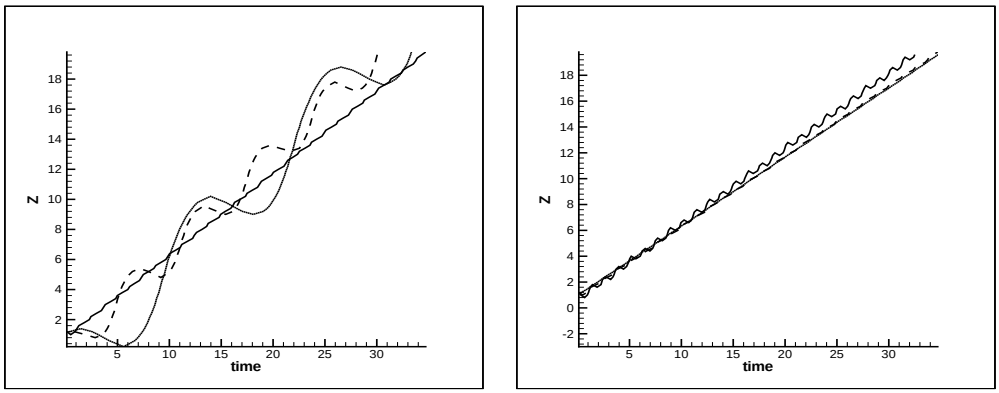

Figure 8: z-coordinate of Maximum Reaction Rate in Domain as a Function of Time for $\overline{D} = 0.750$, $Le_Y = 1.0$, a.) $A = 0.5$, $\omega = 0.5$ (dotted), $\omega = 1.0$ (dashed), $\omega = 5.0$ (solid). b). $\omega = 5.0$, $A = 0.1$ (dotted), $A = 0.5$ (dashed), $A = 1.0$ (solid).

Le=1.0

Flames with equal heat and mass diffusivities are more robust than their small-Le counterparts. For this reason, we do not find the formation of cellular structures for these types of flames regardless of whether the underlying counterflow is steady or oscillatory. Instead, we focus on characterizing the response of the mean edge speed to variations in the amplitude and frequency of oscillation of the time-varying counterflow. For $Le = 1.0$, edge flames can either propagate into the fresh mixture as ignition fronts or retreat back into the burnt gases as failure waves. There exists a value of $\overline{D}$, say $\overline{D}_s$, for which the edge is stationary. Values of $\overline{D} < \overline{D}_s$ result in a failure wave while $\overline{D} > \overline{D}_s$ generates an ignition front. In figure 7, we show that the value of $\overline{D}_s$ depends on both A and ω. We also will discuss the role these parameters play in determining the mean edge speed for both a propagating and retreating flame. An example for a retreating edge flame $\overline{D} = 0.75$ is shown in figure 8. Also, we have found that for sufficiently large ω, the edge flame can persist even when the flame experiences strain larger than the 1-D quenching value for a significant portion of the forcing cycle. This will be discussed in more detail during the presentation of this work.

Acknowledgements

This work was supported by the Air Force Office of Scientific Research (DAK, MS, JB) and by the NASA John H Glenn Research Center at Lewis Field (JB).

References

J. Buckmaster, 1992 "A Flame-string Model and its Stability". *Combust. Sci. Techno.* 84: 167–176.

J. Buckmaster, 2002 "Edge-flames". *Progr. in Energy & Combust. Sci.* 28: 435–475.

T. Echekki and J. Chen, 1996 "Unsteady Strain Rate and Curvature Effects in Turbulent Premixed Methane-Air Flames". *Combust. & Flame* 106: 184–202.

F. Egolfopoulos, 2000 "Structure and Extinction of Unsteady, Counterflowing, Strained, Non-premixed Flames". *Intern. J. of Energy Res.* 24: 989–1010.

Z. Huang, J. Bechtold, and M. Matalon, 1998 "Weakly Stretched Premixed Flames in Oscillating Flows". *Combust. Theo. & Modell.* 2: 115–133.

D. Kessler, M. Short, and J. Buckmaster, 2005 "Edge-flames and Cellular Structures in Oscillatory Premixed Counterflows". *Proceedings of the Combustion Institute* 30.

A. McIntosh, J. Brindley, and X. Yang, 2001 "The Effect of Large Step Pressure Drops on Strained Premixed Flames". *Combust. & Flame* 125: 1207–1216.

M. Short, J. Buckmaster, and S. Kochevets, 2001 "Edge-flames and Sublimit Hydrogen Combustion". *Combust. & Flame* 125: 893–905.

C. Sung and C. Law, 2000 "Structural Sensitivity, Response, and Extinction of Diffusion and Premixed Flames in Oscillating Counterflows". *Combust. & Flame* 123: 375–388.